Lifetime measurement of the Mg I intercombination line

A. Godone and C. Novero
Istituto Elettrotecnico Nazionale Galileo Ferraris, Torino, Italy
(Received 26 November 1990; revised manuscript received 1 April 1991)

The lifetime of the $3s^2\,{}^1S_0$–$3s3p\,{}^3P_1$ intersystem transition of magnesium has been measured by different authors; however, a noticeable discrepancy appears mostly between two groups of measurements. We have measured the $^3P_1$ decay time constant in a metastable atomic beam with a combined laser-microwave excitation technique, based on the 1.5-m downstream detection of the fine-structure transition $^3P_1$-$^3P_0$ (at 601 GHz) with and without laser optical pumping. Due to the decay of the $^3P_1$ state, a population difference between $^3P_1$ and $^3P_0$ levels arises before the interaction of the microwave radiation with the atomic beam allowing the observation of the $^3P_1$-$^3P_0$ magnetic dipole transition; its intensity is then related to the $^3P_1$ decay time constant. Afterwards, the $^3P_1$ state is entirely depopulated through optical pumping just outside the beam exit. The microwave-induced transition intensity in this case is independent of the $^3P_1$ decay constant, with all of the other parameters of the experiment being unchanged. The ratio between the microwave-induced transition probabilities in the two cases is sensibly dependent on the $^3P_1$ lifetime, allowing a determination of its value unaffected by the knowledge of absolute parameters such as atomic flux and detection efficiency, whose evaluation at a sufficient degree of precision may be unreliable. The result of our measurement is $\tau(^3P_1)=5.1\pm0.7$ ms, which is in good agreement with a group of experimental data previously reported in the literature and with theoretical predictions.

PACS number(s): 32.70.Fw, 32.80.Bx

I. INTRODUCTION

The intercombination lines of alkaline-earth metals have been widely considered in the literature due to their spectroscopical and astrophysical interest [1]; the metrological interest for Mg and Ca intersystem lines is more recent: They have been recognized to be good candidates as reference transitions for highly accurate frequency-wavelength standards in the visible region of the electromagnetic spectrum [2]. Moreover, a submillimetric frequency standard, based on the $^3P_1$-$^3P_0$ $\Delta m_j=0$ transition has been developed [3], where the decay of the $^3P_1$ level to ground state along a metastable atomic beam is a natural mechanism for state selection as well as a highly efficient way of detection.

In the fields considered above, the $^3P_1$-$^1S_0$ decay time constant $\tau(^3P_1)$ plays an important role and its value has been estimated theoretically and/or measured experimentally for different alkaline-earth atoms; a problem exists for magnesium: Several authors have measured the $^3P_1$ Mg lifetime, but the reported data lead mainly to two different values, the first centered at about 2 ms [4] and the second at about 5 ms [5].

The deviation from the pure Russell-Saunders coupling (*LS* coupling), due to magnetic interaction that mixes different *LS* states with the same *J* quantum number, is the main origin of the weakly allowed Mg intersystem transition as well as of the Landè anomaly observed for the fine-structure transitions in the $^3P^{(0)}$ term. Even if the Landè anomaly is known with high precision from the frequency measurements reported in [3] and [6]

$$\nu|^3P_2\text{-}^3P_1|/\nu|^3P_1\text{-}^3P_0|=2.029\,971\ ,$$

it is not easily linkable to $\tau(^3P_1)$, at least for the Mg case; an *ab initio* full quantum-mechanical treatment is then required for the theoretical estimation of the $\tau(^3P_1)$ value (see, for example, [7] and references therein).

In this paper, we report an experimental technique to measure the $^3P_1$ decay time constant well suited for the Mg weakly allowed transition, based on a combined laser-microwave excitation method in separated zones of a metastable atomic beam. As will be shown in Sec. II, this technique provides a result that is strongly independent of various parameters such as laser and microwave intensities, radiation patterns, atomic flux, and detection efficiency and sensibly dependent mostly on the $\tau(^3P_1)$ constant, allowing an unambiguous determination of its value.

II. THEORETICAL DESCRIPTION

Let us consider the measurement system shown in Fig. 1. An Mg metastable beam interacts in two separated zones with the radiation of a laser tuned to the $^3S_1$-$^3P_1$ transition frequency and with the submillimetric field in resonance with the $^3P_1$-$^3P_0$ magnetic dipole transition; further downstream, a photomultiplier is used to detect the fluorescence light at 457.1 nm corresponding to the spontaneous decay of the $^3P_1$ level to ground state. We consider now the following cases.

(i) No radiation applied to the atomic beam. In this case a background signal is observed at the photomultiplier (PM) output due to the $^3P_1$-$^1S_0$ natural decay.

(ii) Only the laser radiation interacts with the atomic beam. In this case the atoms in the $^3P_1$ state are optically pumped into the $^3P_0$ and $^3P_2$ states whose transitions to

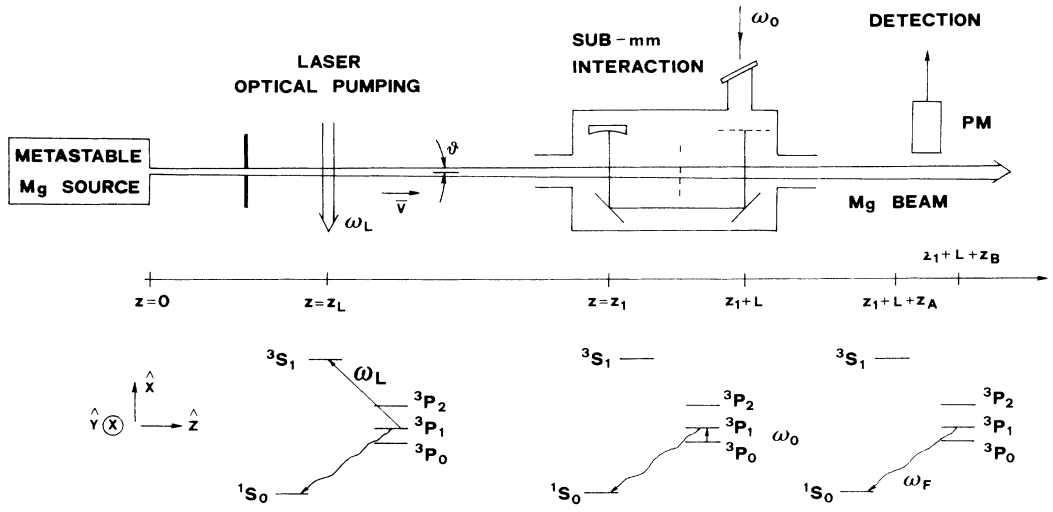

FIG. 1. Schematic representation of the system used for the measurements; relevant Mg energy levels are also reported.

ground level are strongly forbidden: As a consequence, the background signal observed in case (i) is reduced depending on the pumping efficiency.

(iii) Only the submillimeter radiation interacts with the atomic beam. In this case, just before the interaction region a population difference between the $^3P_1$ and $^3P_0$ levels exists due to the $^3P_1$ spontaneous decay: A population inversion is then induced after the interaction with the submillimeter field that increases the fluorescence signal observed at the PM output by a quantity related to the preexisting population difference.

(iv) Both the laser and the submillimeter radiations interact with the atomic beam. In this case the background signal is reduced as in case (ii) and the signal induced by the submillimeter radiation increases with respect to case (iii) due to the larger population difference produced by the laser optical pumping.

The ratio between the two signals induced by the submillimeter radiation in cases (iv) and (iii) is related to $\tau(^3P_1)$ in a definite way; the relation between the two quantities is deduced in the following part of this section.

Let us consider the change $S(\Omega)$ of the fluorescence signal induced by the submillimeter radiation; it may be expressed in the following way (see also [8]):

$$S(\Omega)=\frac{\Theta}{4\pi}\frac{2}{9}\eta\Phi_0\hbar\omega_F\mathcal{R}\langle P(\Omega)\rangle \ , \tag{1}$$

where Θ is the photocathode observation solid angle, η is the efficiency of production of metastable atoms, Φ_0 is the atomic flux (atoms s^{-1}) in the ground state at the collimator output, $\hbar\omega_F$ is the energy of the fluorescence photon, $\mathcal{R}$ is the PM responsivity (V W^{-1}), $\langle P(\Omega)\rangle$ is the transition probability induced by the submillimeter radiation, and $\Omega=\omega-\omega_0$ is the detuning between the submillimeter frequency ω and the atomic transition frequency.

The ratio between the signals observed in case (iv), $S_2(\Omega)$, and in case (iii), $S_1(\Omega)$, is given by

$$\frac{S_2(\Omega)}{S_1(\Omega)}=\frac{\langle P(\Omega)\rangle_2}{\langle P(\Omega)\rangle_1} \ . \tag{2}$$

The left-hand-side ratio of Eq. (2) may be measured with good resolution in the experiments (better than 5%) and depends only on the induced transition probabilities evaluated with and without optical pumping. The expression of $\langle P(\Omega)\rangle$ may be written as follows [9]:

$$\langle P(\Omega)\rangle=\int_\theta\int_A\int_v f(\theta)\Gamma_\theta(v)\rho_m(v) \times(e^{-(z_A)/(\tau v)}-e^{-(z_B)/(\tau v)}) \times\Delta(R_3^{(f)}+R_4^{(f)})d\theta\, d\sigma\, dv \ , \tag{3}$$

where $f(\theta)$ is the normalized angular profile of the atomic beam; $\Gamma_\theta(v)$ is the deformation function [10], which takes into account the possible angular dependence of the velocity distribution; $\rho_m(v)$ is the velocity distribution of the metastable atoms [11];

$$\Delta(R_3^{(f)}+R_4^{(f)})=(R_3^{(f)}+R_4^{(f)})\omega_R-(R_3^{(f)}+R_4^{(f)})\omega_{R=0} \ ,$$

with ω_R the Rabi angular frequency; $R_3^{(f)}, R_4^{(f)}$ are two components of the Block vector as defined in [8] and [9] just at the end of the interaction region; and A is the section of the atomic beam.

The expressions of the Bloch vector components for the submillimeter interaction in the Ramsey cavity have been derived in [8] and [9] in the case $\Omega=0$ and omitting the effect of the decay constant τ in the single interaction zone; the first hypothesis is of no importance for our experiment while the second one requires $\tau(^3P_1)\gg 2\rho_0/v$, with $2\rho_0$ the e^{-1} diameter of the Gaussian field intensity inside the electromagnetic cavity.

The two cases of interest for this work, laser optical pumping "on" and "off," define two different "initial conditions" before the interaction region; starting from expression (3), with the use of the formalism reported in [9], a straightforward computation leads to the following expression:

$$\frac{\langle P(0)\rangle_2}{\langle P(0)\rangle_1}=\frac{\int_\theta\int_A\int_v f(\theta)\Gamma_\theta(v)F_\rho(v)(1+\frac{1}{2}e^{-(z_L/\tau v)})\sin^2\zeta\, d\theta\, d\sigma\, dv}{\int_\theta\int_A\int_v f(\theta)\Gamma_\theta(v)F_\rho(v)\left[(1-e^{-(z_1/\tau v)})\sin^2\zeta+4e^{-(z_1/\tau v)}\left[\tanh\frac{L}{4\tau v}\right]\sin^2\frac{\zeta}{2}\right]d\theta\, d\sigma\, dv}\ , \tag{4}$$

where

$$F_\rho(v)=(e^{-(z_A)/(\tau v)}-e^{-(z_B)/(\tau v)})(1+e^{-L/(2\tau v)})^2\rho_m(v)$$

and

$$\zeta=\frac{\sqrt{2\pi}\omega_R\rho_0}{v}\frac{e^{-(1/2)(\beta\rho_0\tan\theta)^2}}{\cos\theta}e^{-y^2/2\rho_0^2}\cos\beta x\ ,\quad \beta=\frac{2\pi}{\lambda}\ .$$

z_A, z_B, L, z_1, and z_L are defined in Fig. 1.

The expression of ζ is written for a TEM_{00q} Gaussian field inside the cavity with a standing wave along the $\hat{x}$ direction. A Boltzmann distribution for the metastable levels has been assumed in deriving Eq. (4). Expression (4) simplifies in the low-field case ($\omega_R\to 0$) and for $\Gamma_\theta(v)\sim 1$ (we will reconsider this hypothesis in Sec. III), leading to

$$\lim_{\omega_R\to 0}\frac{\langle P(0)\rangle_2}{\langle P(0)\rangle_1}=\frac{\int_0^{+\infty}\frac{1}{v^2}F_\rho(v)[1+(1/2)e^{-(z_L/\tau v)}]dv}{\int_0^{+\infty}\frac{1}{v^2}F_\rho(v)\left[1-e^{-(z_1/\tau v)}\left[1-\tanh\frac{L}{4\tau v}\right]\right]dv}\ . \tag{5}$$

Equation (5) is independent of the submillimeter field coupled to the cavity and of the laser field, when applied, provided the optical pumping completely depletes the $^3P_1$ state before the interaction region; Eq. (5) depends only on the geometrical parameters of the experimental setup and on the metastable atom velocity distribution $F_\rho(v)$; the two factors enclosed between square brackets in the numerator and denominators are related to the population difference between the $^3P_{1,m_j=0}$ and $^3P_0$ levels with and without optical pumping, respectively.

III. EXPERIMENTAL SETUP AND RESULTS

The source of metastable atoms used in this experiment is the same described in [11]; the Mg atoms effuse from an oven operating at 520 °C and are excited to the metastable triplet via collision with low-energy electrons. The total beam divergence after collimation is $\Delta\theta=10$ mrad, the total atomic flux in the beam is $\Phi_0\simeq 4\times 10^{13}$ atoms s^{-1}, and about 40% of them are in the ^3P states at the optimum discharge current. The velocity distribution of the metastable atoms is given by

$$\rho_m(v,I)=A\left[\frac{v}{\alpha}\right]^\gamma e^{-(HI)/v-v^2/\alpha^2}\sinh\left[\frac{KI}{v}\right]\ , \tag{6}$$

where A is a normalization constant; α is the most probable velocity in the oven; γ is a positive number higher than 3, which takes into account the elastic collision effect; I is the discharge current; and H and K are constants dependent on the excitation and deexcitation cross sections of Mg and on the discharge geometry.

For our source the following values apply: $\alpha=736$ ms^{-1}, $\gamma=4.5$, $H=2200$ $ms^{-1}A^{-1}$, $K=1540$ $ms^{-1}A^{-1}$. The wavelength of the optical pumping transition, in resonance with the $^3S_1$-$^3P_1$ Mg transition, is $\lambda=517.4$ nm ($\tilde{\nu}=19\,326.935$ cm^{-1}); it is generated by a Coumarin 6 ring dye laser, pumped by the 488-nm emission of the Ar^+ laser, and frequency locked to an external reference cavity. The laser interaction region is at a distance $z_L=0.5$ m downstream from the atomic source; further details regarding the polarization of the laser beam and the efficiency of the optical pumping of the metastable states of Mg may be found in [12].

The interaction between the Mg atoms and the submillimeter radiation is obtained via a Ramsey cavity (doubly folded open resonator) with a spatial selector of the atomic trajectories as described in [3]; the distance between the first interaction region and the atomic source is $z_1=1.11$ m and the Ramsey cavity length is $L=30$ cm. The submillimeter source is a backward-wave oscillator (BWO) phase-locked to a high spectral purity quartz oscillator via a low phase-noise frequency multiplication chain; the $^3P_1$-$^3P_0$ $\Delta m_j=0$ transition frequency of ^{24}Mg is $\omega_0/2\pi=601\,277\,157\,860\pm 20$ Hz [3]. The PM detects the intercombination fluorescence light ($\lambda=457.1$ nm) emitted in the region between $z_A=0.5$ m and $z_B=0.7$ m from the second interaction zone.

The record of the ^{24}Mg $^3S_1$-$^3P_1$ transition is shown in Fig. 2: It is the PM output when the laser frequency is scanned in the absence of the submillimeter radiation [case (ii) of Sec. II]; the ^{26}Mg transition and some ^{25} Mg hyperfine-structure transitions are observed as well. The decrease of the $^3P_1$ fluorescence light for the ^{24}Mg atoms corresponds to a nearly full optical pumping of the $^3P_1$ state, as required to derive Eq. (5); the laser power density is 15 mW/cm^2. In Fig. 2 the baseline level of the resonances is the fluorescence signal due to the natural decay of the $^3P_1$ atoms when no radiation is applied.

When the dye laser is tuned to the $^3S_1$-$^3P_2$ transition frequency, the ^{24}Mg fluorescence signal is enhanced by a factor of 2.1, in agreement [12] with the hypothesis of a

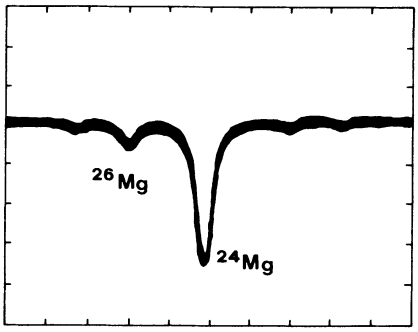

FIG. 2. $^3S_1$-$^3P_1$ Mg transition observed through the 457.1-nm fluorescence light; horizontal 200 MHz/div; vertical, 200 mV/div; video bandwidth, 10 kHz.

Boltzmann distribution of the atomic population in the metastable triplet, as assumed in the derivation of Eq. (4). The Ramsey signal, detected at the PM output, corresponding to the $^3P_1$-$^3P_0$ $\Delta m_j=0$ transition of ^{24}Mg is shown in Fig. 3 with and without optical pumping [cases (iv) and (iii) of Sec. II, respectively]; the above signals have been tested to be proportional to the submillimeter power coupled to the cavity, in order to satisfy the hypothesis $\omega_R \to 0$ required to obtain Eq. (5). The vertical axis of Fig. 3 is normalized to the peak value ($\Omega=0$) of the signal in the absence of the laser pumping power and then coincides with the left-hand-side ratio of Eq. (5); the discharge current is $I=300$ mA.

The experiment has been repeated for different current settings: The ratio between the peak amplitudes of the Ramsey fringes versus the discharge current is reported in Fig. 4, where each point is the mean of nine measures with an absolute standard deviation of ± 0.2. The continuous curves are obtained from a numerical evaluation of Eq. (5), having assumed for the parameters of the velocity distribution the values reported in this section; the curve corresponding to $\tau=5.1$ ms represents the best fit for the experimental data.

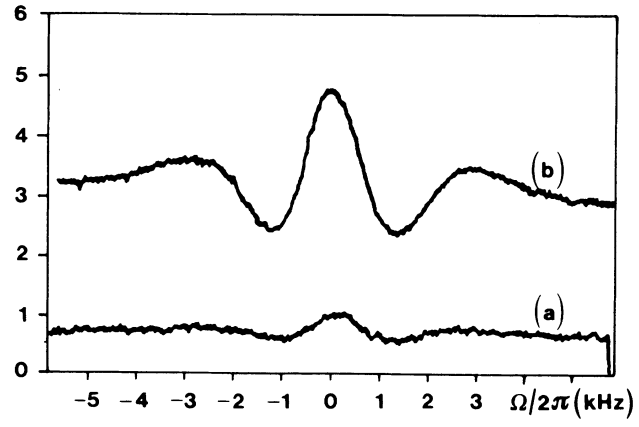

FIG. 3. $^3P_1$-$^3P_0$ $\Delta m_j=0$ Ramsey signal for ^{24}Mg. (a) Without optical pumping; (b) with optical pumping. The vertical axis is normalized to the peak value of curve (a) $\Omega/2\pi=0 \to \nu_0=601\,277\,157\,860$ Hz.

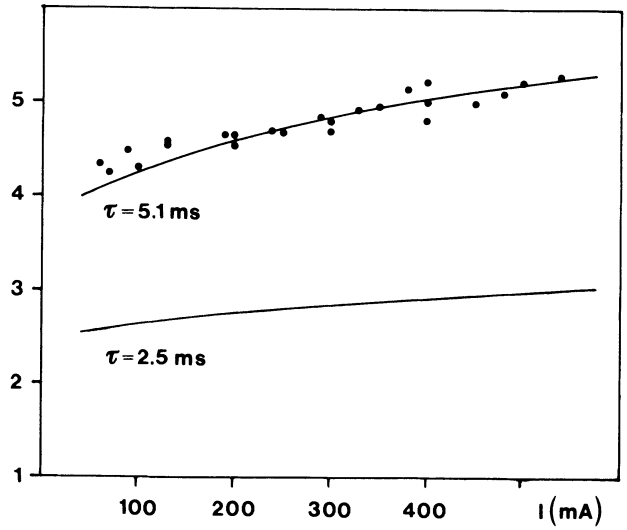

FIG. 4. Ratio between the peak amplitudes of the Ramsey fringes with and without optical pumping vs the discharge current. ●, experimental values; ——, theoretical evaluation.

IV. DISCUSSION OF THE RESULTS

The value of the decay time constant $\tau(^3P_1)$ is deduced from the experimental results via Eq. (5), which relies on the following main hypotheses: Submillimeter low interaction field ($\omega_R \to 0$); full optical pumping of the $^3P_1$ state; Boltzmann distribution for the $^3P_{0,1,2}$ states; atom transit time negligible with respect to the $^3P_1$ decay constant in each interaction region: $2\rho_0/v \ll \tau(^3P_1)$; and axial velocity distribution uniform in the atomic beam section: $\Gamma_\theta(v)=1$.

As far as the first four hypotheses are concerned, they are widely satisfied by the experimental arrangement, as noted in Sec. III. In order to satisfy the last hypothesis, we have avoided operating at high discharge current levels ($I \leq 500$ mA) to reduce possible velocity-dependent diffusion processes in the region of production of the metastable beam, moreover, no significant change in the experimental results has been observed changing the beam divergence from 10 to 25 mrad.

Furthermore, quenching effects of the ^3P_J states have not been observed in the pressure range $1-5\times10^{-7}$ Torr, in agreement with the collision deexcitation cross section reported for the metastable Mg states ($\sigma^2<1$ Å^2 at 300 K [13]). The absence of systematic quenching effects, moreover, is also proved by the measured efficiency of production of metastable atoms (40%) in agreement with the theoretical value expected from the excitation and deexcitation cross sections of the ^3P states [11]. Our result is then unaffected by the vacuum level of the experimental apparatus or from Mg gas in the $^1S_0$ ground state due to partial reflection of the atoms from the collimators and from the end of the vacuum chamber.

The main source of uncertainty in the application of Eq. (5) to derive the $\tau(^3P_1)$ value is then related to the knowledge of the metastable atom velocity distribution: Allowing a fluctuation range of $\pm 10\%$ for the parameters H, K, and γ around the nominal values reported in [11],

an uncertainty of ± 0.5 ms turns out for the estimated value. Taking into account the experimental uncertainty and reproducibility of the measurements, we assume a total conservative uncertainty of ± 0.7 ms; then

$$\tau(^3P_1) = 5.1 \pm 0.7 \text{ ms}$$

or

$$A = \tau^{-1} = (1.9 \pm 0.3) \times 100 \text{ s}^{-1} .$$

This result is in good agreement with the theoretical [7] and experimental [5] values reported in the literature.

Furthermore, it must be remarked that the experiments for the magnesium atom reported in [4] are not in contrast with the present value if they are refitted with the velocity distribution reported in [11]. In fact, in [4] the following velocity distribution has been guessed (modified Maxwellian) for the metastable atoms:

$$\rho(v) = c \left[\frac{v}{\alpha} \right]^{\beta} e^{-v^2\alpha^2} , \tag{7}$$

with $\beta = 5-7$, instead of (6). The above relation (7) does not take into account the dependence of the velocity distribution of the metastable atoms on the discharge current I, giving rise to a "significant decrease in the measured lifetime when the current changes from 75 to 250 mA", as noted in [4].

At the relatively low current values used in [4], relation (6) gives

$$\rho_m(v) \simeq \overline{A} \left[\frac{v}{\alpha} \right]^{\gamma-1} e^{-v^2/\alpha^2} ,$$

corresponding to (7) with $\beta = \gamma - 1 \simeq 3$; if this value is inserted in Eq. (5) of Ref. [4], the lifetime turns out to be $\tau = 4.2 \pm 0.3$ ms, in much better agreement with our measurements.

As a concluding remark, the main feature of the technique described in this work is that the final result is strongly independent of absolute parameters such as atomic flux, field intensities, atomic and electromagnetic beam profiles, detection system, stray light from discharge or laser, etc., whose evaluation at a sufficient degree of precision may be difficult from an experimental point of view, or unreliable, and relies mainly on the knowledge of the velocity distribution of the metastable atoms, which has been measured with a precision level high enough for this purpose.

[1] R. H. Garstang, J. Opt. Soc. Am. **52**, 845 (1962).
[2] W. Ertmer, R. Blatt, and J. L. Hall, Prog. Quantum Electron. **8**, 249 (1984).
[3] A. Godone, E. Bava, and C. Novero, Metrologia **24**, 133 (1987).
[4] G. Boldts, Z. Phys. **150**, 205 (1958); G. Giusfredi, P. Minguzzi, F. Strumia, and M. Tonelli, Z. Phys. A **274**, 279 (1975).
[5] C. J. Mitchell, J. Phys. B **8**, 25 (1975); P. S. Furcinitti, J. J. Wright, and L. C. Balling, Phys. Rev. A **12**, 1123 (1975); H. S. Kwong, P. L. Smith, and W. H. Parkinson, *ibid.* **25**, 2629 (1982).
[6] M. Inguscio, K. R. Leopold, J. S. Murray, and E. M. Evenson, J. Opt. Soc. Am. B **2**, 1566 (1985).
[7] C. Laughlin and G. A. Victor, Astrophys. J. **234**, 407 (1979).
[8] E. Bava, A. Godone, and G. Rietto, Appl. Phys. B **41**, 187 (1986).
[9] E. Bava, A. Godone, and C. Novero, Appl. Phys. B **48**, 495 (1989).
[10] H. C. W. Beijerinck and N. F. Verster, J. Appl. Phys. **46**, 2083 (1975).
[11] G. Giusfredi, A. Godone, E. Bava, and C. Novero, J. Appl. Phys. **63**, 1279 (1988).
[12] A. Godone, C. Novero, and E. Bava, IEEE Trans. Instrum. Meas. **40**, 149 (1991).
[13] R. P. Blickensderfer, W. H. Breckenridge, and D. S. Moore, J. Chem. Phys. **63**, 3681 (1975).